Faraday Discussions

Accepted Manuscript

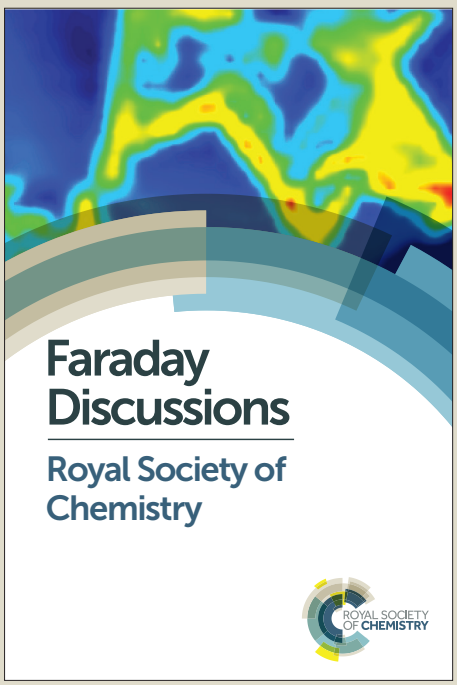

This article can be cited before page numbers have been issued, to do this please use: S. Ramalhete, J. S. Foster, H. R. Green, K. P. Nartowski, M. Heinrich, P. Martin, Y. Z. Khimyak and G. O. Lloyd, *Faraday Discuss.*, 2017, DOI: 10.1039/C7FD00108H.

View Article Online
DOI: 10.1039/C7FD00108H

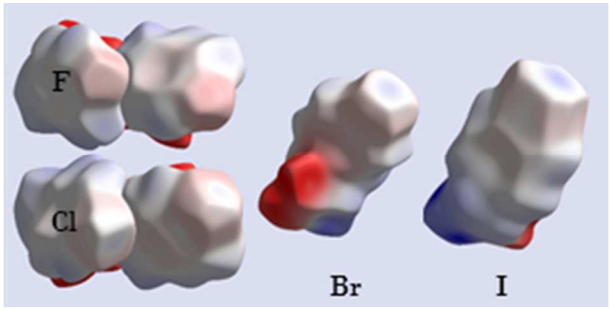

Journal Name

View Article Online
DOI: 10.1039/C7FD00108H

ARTICLE

Halogen effects on the solid-state packing of phenylalanine derivatives and the resultant gelation properties

Received 00th January 20xx,
Accepted 00th January 20xx

DOI: 10.1039/x0xx00000x

www.rsc.org/

Susana M. Ramalhete,[a] Jamie S. Foster,[b] Hayley R. Green,[b] Karol P. Nartowski,[a] Margaux Heinrich,[b] Peter C. Martin,[c] Yaroslav Z. Khimyak[a*] and Gareth O. Lloyd[b*]

Phenylalanine is an important amino acid both biologically, essential to human health, and industrially, as a building block of artificial sweeteners. Our interest in this particular amino acid and its derivatives lies with its ability to form gels in a number of solvents. We present here the studies of the influence of halogen addition to the aromatic ring on the gelation properties and we analyse the crystal structures of a number of these materials to elucidate the trends in their behaviour based on the halogen addition to the aromatic group and the interactions that result.

Introduction

Phenylalanine (Phe) is the amino acid that has produced an extra-ordinary set of scientific insights in the last half decade. Numerous new crystal structures, polymorphs, hydrates and gel forms have peaked research interest in its solid-state behaviour the world over.[1] Coupled to this is the fact that Phe is a key component in the synthesis of natural and synthetic products such as aspartame, peptides and medicines. Our primary interest is in the gelation properties of the compound and its derivatives. A gel is a colloidal material in which a gelator is dispersed (the solid, continuous phase) within a solvent (the liquid, dispersed phase). Aggregation of phenylalanine in water has recently been linked to the disease phenylketonuria[1a] and the solid state form of those fibres of the gels have been elucidated to be the monohydrate crystal form, which was first characterised by Harris and co-workers.[1k] As well as the hydrogel formation, we have also shown that Phe forms gels with DMSO.[1p] Phe is one of the smallest molecules yet known to form a gel. With this in mind, we turned to the question of how to improve its gelation properties, e.g. to lower critical gel concentrations (CGCs), and to direct rheological properties. As a first step, we decided to change the aromatic portion of the Phe molecule by adding halogen groups. The reasoning behind this lies in our initial understanding of the self-assembly of Phe. With a number of potential sites for interactions within the molecule, namely π-π interactions, hydrogen bonding, hydrophobic effects and electrostatic interactions between the zwitterionic components of the compound, there are a number of chemical modifications that can be implemented to affect the resulting gelation properties. However, our studies of the Phe gelation highlighted that the electrostatic interactions dominate the self-assembly process and that removal of these prevents gelation. The hydrophobic effects, C–H···π and π-π interactions provide a minor contribution to stabilisation of the three-dimensional crystal structure and therefore have a subtler effect on gelation processes.[1p] Hence, we felt this was the most appropriate chemical functionality to alter, that would affect the tuning of the gelation properties of Phe without totally disrupting the gelation.

The study of halogenation of Phe, or of Phe as a molecular building block of the compound, has resulted in a number of interesting results. These included, but are not limited to, the following findings. A crystal structure analysis of four fluorinated Phe compounds by In and co-workers reveal that there are generally familiar features to the supramolecular packing.[2] These are the bilayer motif of a hydrophobic layer and hydrophilic layer, and that the degree of fluorination can alter the interactions between the phenyl rings. However, we note that there are two hydrates and two anhydrous forms discussed. We will present analysis of only the monohydrate forms of the derivatives for more palpable trends to be ascertained. Halogenation of fluorenylmethyloxycarbonyl-Phe (FMOC-Phe) derivatives by Ryan et al. (2010) and Pizzi et al. (2017) showed that self-assembly processes in water and the mechanical properties of the resulting materials were highly dependent on halogen identity and substitution position on the aromatic ring.[3] An important aspect to take into account in all these studies is the concept of the halogen – halogen interaction and halogen bonding.[4] This has been utilised in a number of studies involving small molecule gelators.[5] In

[a] School of Pharmacy, University of East Anglia, Norwich, United Kingdom, NR4 7TJ, E-mail: Y.Khimyak@uea.ac.uk.
[b] Institute of Chemical Sciences, School of Engineering and Physical Sciences, Heriot-Watt University, Edinburgh, Scotland, United Kingdom, EH14 4AS, E-mail: G.O.Lloyd@hw.ac.uk
[c] Department of Chemistry, Cambridge University, Lensfield Road, Cambridge, United Kingdom, CB2 1EW.
† Footnotes relating to the title and/or authors should appear here.
Electronic Supplementary Information (ESI) available: [details of any supplementary information available should be included here]. See DOI: 10.1039/x0xx00000x

particular, the Br and I derivatives can often show significant halogen-based interactions that cause a stepped change in structural packing and properties.[3-5] Fluorination of biologically active compounds is of particular interest due to the use of ^{18}F in positron emission tomography (PET) scanning.[6] There have been a number of studies of fluorinated Phe for this particular reason and for other medicinal applications. However, little or no information is known on the effect this has on the self-assembly of Phe derivatives in water and other solvents.

The gelation properties of a number of chirally pure Phe derivatives (Fig. 1) were thus determined. These are: 4-fluorophenylalanine (F-Phe), 3,4-difluorophenylalanine (2F-Phe), pentafluorophenylalanine (5F-Phe), 4-chlorophenylalanine (Cl-Phe), 3,4-dichlorophenylalanine (2Cl-Phe), 4-bromophenylalanine (Br-Phe), and 4-iodophenylalanine (I-Phe). As well as the gelation properties investigated via morphology determination, rheology, and NMR spectroscopy, we also determined crystal structures for a number of these compounds and analysed the structures crystallographically.

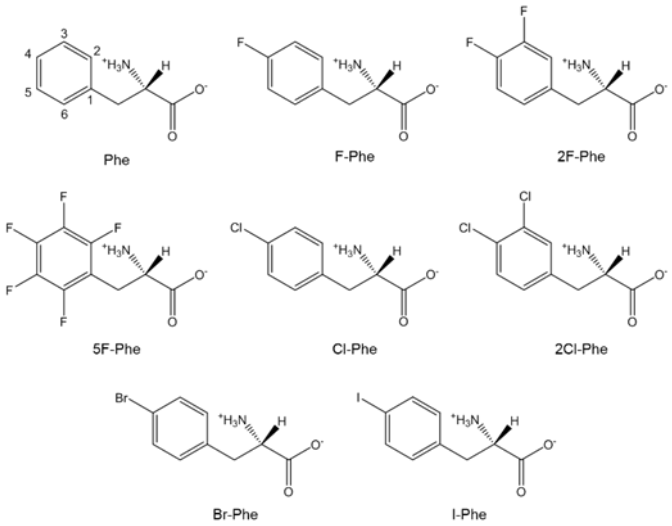

Fig. 1. Chemical structure of Phe with numbering of aromatic carbon atoms and Phe halogenated derivatives used in the study.

Experimental

Materials

Methods. Chemicals were purchased from the following companies and used without further purification: *L*-phenylalanine (Phe) – Sigma Aldrich, halogenated Phe supplied by Fluorochem; DMSO – Fisher; deuterated solvents (D_2O, DMSO-d6) – Goss Scientific. We note that, in most cases, there must be some care taken with commercial samples of the derivatives of Phe as they are not always sufficiently pure to allow for the gelation properties to be reproducible.

Gelation procedures. All gels are heat set/thermoreversible gels. Gelation tests were performed by dissolving the amino acids in DMSO (anhydrous) or distilled water in screw cap glass vials under a heat gun. Setting of the gels was initiated by cooling, often under a cold water tap. Some gelation was noted when the materials were sonicated hot or just upon mixing. Sonication often resulted in more homogeneous samples when compared to vials that were left on a bench undisturbed.

Crystallography and crystal structure analysis. Crystals were selected from the fibres found in the hydrogel formation experiments or synthesised utilising MeOH or EtOH as co-solvents. The co-solvent method often resulted in slightly larger single crystals. Selected crystals were mounted on to cryo-loops utilising Paratone® oil. Crystals were crash cooled under a N_2 cryostream. Data was collected utilising two instruments, an Agilent Xcalibur Eos Gemini ultra, and a Bruker APEX-II CCD. The crystal structures were solved utilising Shelx interfaced into Xseed or Olex2. Electrostatic potential Hirshfeld surfaces were calculated using CrystalExplorer with Tonto. DFT calculation was performed with 6-311G (d,p) basis set with Becke88 exchange potential and LYP correlation potential. Images were generated utilising Xseed or CrystalExplorer.

Rheology. Rheological experiments were performed on a Bohlin nano II rheometer. All samples were collected using a gap of 200 µm and a solvent trap. Two different methods were utilised for measurements. The rheometer was equipped with a 40 mm stainless steel cone (4°) or a 40 mm acrylic plate. It was found that the cone and plate gave comparable results for these materials. Gels for rheological analysis were formed as follows. In a sealed vial containing 2 ml of solvent the appropriate amount of the Phe derivative was dissolved with the aid of heating. Once fully dissolved the solution was injected into the gap between the cone and the rheometer's plate (50 or 20 °C) using a warmed syringe. Once the solution was in place the plate was gradually cooled to 20 °C or left at 20 °C. These materials were left for up to 1 h to allow the gel to completely form.

Scanning electron microscopy (SEM). SEM images were produced using a FEI Quanta 3D SEM equipped with an Everhart Thornley Detector (ETD) operating in high vacuum mode. The electron source is a field emission gun (FEG) operating at 5 kV accelerating voltage. A second instrument was also utilised. It is a Philips XL30 LaB6 ESEM equipped with an Oxford Instrument X-max 80 EDX detector at 3 kV. Wet gel samples were placed on carbon sticky tabs mounted on aluminium SEM stubs. Once mounted, samples were dried under vacuum in a desiccator for 48 hours. These dried samples were then gold coated for 20 seconds at 20 µA or 2 minutes at 12 µA using a sputter coater.

Nuclear Magnetic Resonance (NMR) Spectroscopy.

Solid-state NMR spectroscopy. Solid-state NMR experiments were carried out using a Bruker Avance III NMR spectrometer operating at frequencies of 400.23 MHz (^1H) and 100.64 MHz (^{13}C), equipped with a 4 mm wide bore probe. Dried gel samples were packed directly into 4 mm zirconia rotors. ^1H-^{13}C CP/MAS

NMR spectra of dried samples were acquired using 2048 scans, a recycle delay of 20 s, a contact time of 2 ms and an MAS rate of 10 kHz. ^{1}H and ^{13}C spectra were referenced to tetramethylsilane (TMS). All experiments were conducted at 298 K.

Solution-state NMR spectroscopy. Solution-state NMR experiments were performed using a Bruker Avance I spectrometer operating at a frequency of 499.69 MHz (^{1}H) equipped with a 5 mm triple resonance probe. 600 µL hot solutions were pipetted into NMR tubes and allowed to form a gel inside. ^{1}H-NMR spectra were acquired using excitation sculpting for water suppression (zgespg) with a recycle delay of 10 s. ^{1}H longitudinal relaxation times (T_1) were measured using a standard inversion recovery pulse sequence with a recycle delay of 10 s. 16 points were recorded at variable time delays ranging from 0.1 to 20 s. The evolution of intensities were fitted mathematically to the mono-exponential function $M_z(\tau) = M_0 * \left[1 - e^{\left(\frac{-\tau}{T_1}\right)}\right]$, where M_z is the z-component of magnetisation, M_0 is the equilibrium magnetisation and τ is the time delay.[7] All experiments were conducted at 298 K.

Results and Discussion

Gelation properties

In order to understand the effect of the addition of halogens to the aromatic functionality of Phe on the self-assembly of the Phe derivatives, we investigated gelation performance in water and DMSO. Seven halogenated Phe derivatives (Fig. 1) were tested and the majority were found to gel in both water and DMSO, as has been observed for the parent compound Phe (Fig. 2). The only significant difference noted was for Br-Phe and I-Phe. I-Phe was found not to gel in the solvents tested. In the case of Br-Phe, the compound was found to gel, however, these gels were found to be very metastable. This behaviour is different to that found with the FMOC-Phe derivatives, where gelation still occurs with Br and I derivatives.[3] Generally, the DMSO gels were found to transform from the clear and transparent gel states to fine white precipitates over a few days. The water gels formed opaque, fibrous gels, which transformed over a day into a fibrous crystalline material that no longer survived the "inversion" test. The determination of the critical gel concentration (CGC) via this "inversion" test showed a general decrease of the CGC value with increasing molecular mass of Phe derivatives for both the hydrogel and organogel series (Table 1). Despite the lowering of the molar CGC trends with the increase of molecular weight, the CGC values as % of weight/volume only decreases slightly. Generally, a more hydrophobic group also decreases the CGC, as shown in the FMOC-Phe series of compounds.[3]

There is current interest within the supramolecular gel community to correlate some form of parametrised "solubility" with the propensity of a compound to form a gel.[8] We therefore compared the Hansen solubility parameters (δ_d; δ_p; δ_h) of DMSO and water, which account for dispersion forces (δ_d), dipolar intermolecular forces (δ_p) and hydrogen bonds (δ_h) between molecules.[9] On first inspection (Fig. 3), the parameters appear to be quite similar, δ_d 15.5 for water and 18.4 for DMSO, δ_p 16 for water and 16.4 for DMSO. However, the δ_h values are significantly different for this pair of solvents, 42.3 for water and 10.2 for DMSO. This difference indicates that these two gels, H_2O and DMSO, should not be related to each other.

Table 1. Gelation results for Phe and its derivatives utilising H_2O and DMSO as solvents.

Compound	Product	CGC in H_2O (M)	CGC in DMSO (M)	Rheology (G') H_2O*:DMSO# (Pa)
Phe	Gels	0.18	0.03	121K:27K
F-Phe	Gels	0.16	0.043	210K:10K
2F-Phe	Gels	0.14	0.04	200K:12K
5F-Phe	Gels	0.08	0.013	250K:8K
Cl-Phe	Gels	0.10	0.025	215K:8K
2Cl-Phe	Gels	0.085	0.02	3K:10K
Br-Phe	Metastable Gels	0.04	0.03	73K:30K
I-Phe	Insoluble/precipitation	-	-	-

* = 3 % by weight/volume. # = 1 % by weight/volume

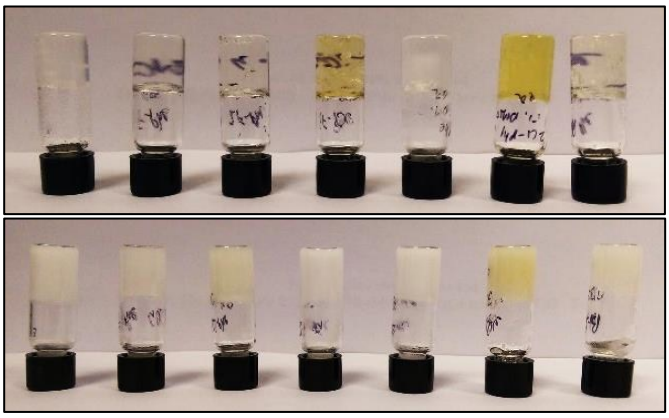

Fig. 2. Photographs of the gels of Phe and its derivatives in water (below) and DMSO (above). From left to right, images are of Phe, F-Phe, 2F-Phe, 5F-Phe, Cl-Phe, 2Cl-Phe, and Br-Phe. All gels were set a 3 % by weight/volume in water, except for Phe, which was at 3.5 % by weight/volume, and 1 % by weight/volume in DMSO.

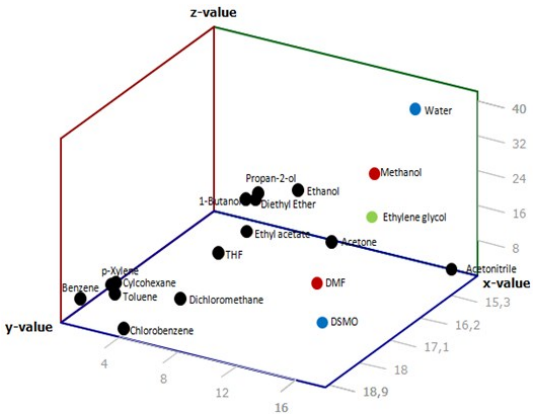

Fig. 3. Solubility data for Phe (at 1 % by weight/volume), represented in Hansen space. The gels are represented by blue points, the formation of a precipitate after full dissolution by red points, a solution by the green point and insoluble/partly soluble in a solvent by black points. X-value is δ_p, Y-value is δ_d, and the Z-value is δ_h.

Other physical measurements reveal that by visual inspection there are opaque hydrogels and transparent DMSO gels (Fig. 2), the rheological properties of the two types of gels are significantly different, and the CGCs for the two solvents are notably dissimilar (Table 1). As well as these characteristics we will show the hydrogels are crystalline in nature and the organogels are not. This trend was recently described for the parent compound Phe.[1p]

SEM and Morphology

The morphology of the gels was assessed by performing SEM on dried samples. The images of the hydrogels gave clear fibrous morphology (Fig. 4). The size of these fibres was found to be in the scale of 600-2000 nm wide, which is consistent with the fact that the gels are opaque and that the fibrous nature can be observed with the visible eye. The DMSO gels, however, are transparent and clear. The fibrous nature could be confirmed from the SEM images (Fig. 5), with fibres found to be significantly thinner (70-212 nm wide), even to the point where it was difficult to discern the size with the resolution possible for the samples and instruments. It was difficult to capture the transient nature of the Br-Phe materials due to a phase transition of the material upon drying.

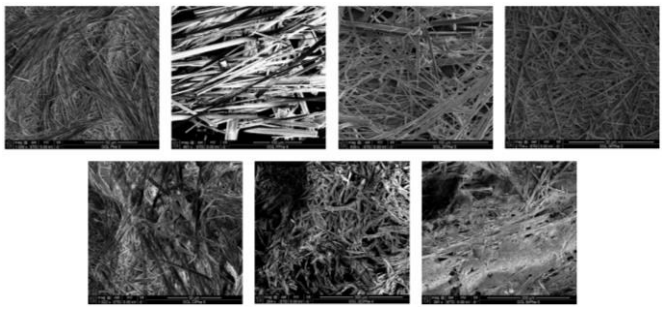

Fig. 4. SEM images of hydrogels of Phe and the halogenated Phe compounds. From top left, images are of Phe, F-Phe, 2F-Phe, 5F-Phe, Cl-Phe, 2Cl-Phe and Br-Phe. All gels were set a 3 % by weight/volume, except for Phe, which was at 3.5 % by weight/volume. These images confirm the presence of large fibres, known to be crystalline, of the gelatinous materials.

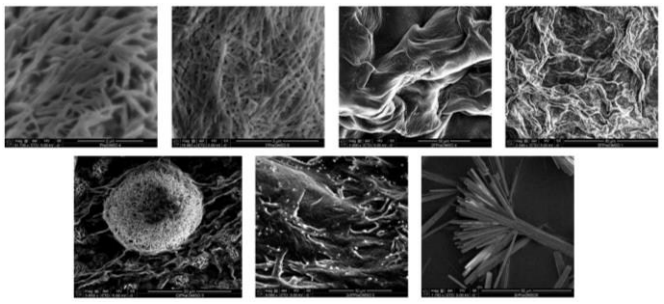

Fig. 5. SEM images of DMSO gels of Phe and the halogenated Phe compounds. From top left, images are of Phe, F-Phe, 2F-Phe, 5F-Phe, Cl-Phe, 2Cl-Phe, and Br-Phe. All gels were set a 1 % by weight/volume. The fibrous nature of the materials after drying can be noted. The Br-Phe always appears to phase change upon drying, resulting in images of the crystalline Br-Phe material.

Rheology

All the gels were characterised by rheology to ascertain firstly their viscoelastic nature, and secondly the variation, if any, in the gel properties. When frequency sweeps were performed with a small amplitude stress (Figs. S1 and S2), on a number of different samples varying in concentration, the solid-like nature at 20 ˚C was reflected in the storage modulus, *G'*, being typically two to five times greater than the loss modulus, *G''*. This demonstrated the elastic behaviour of the gels formed in both solvents. This viscoelastic behaviour is associated with classical gels. This, therefore, supports the notion that the cooling of these samples from a solution to a solid-like material resulted in a true gel state.[10]

Comparison of the rheological values from the analyses indicates that all the DMSO gel materials are comparable, with the *G'* values within a magnitude of order of each other. This was certainly evident when handling the gels with a spatula, with the materials generally keeping shape and being difficult to compress. In comparison, the hydrogels would often collapse under mechanical manipulation with a spatula, extruding the majority of the water. However, the rheology behaviour of hydrogels is significantly different from that of the DMSO gels, in that the *G'* values are at least a magnitude of order higher than those of organogels. The larger size of the fibres and crystalline rigidity of the hydrogels in comparison to the organogels can partly explain this behaviour. The trend of lowering the CGC within the hydrogels upon addition of the halogenated groups to the Phe derivatives is partly matched by the trends in the *G'* values. The *G'* values increase with increase in the F addition from F-Phe to 2F-Phe, and finally 5F-Phe. This can be partly explained again by the concentration of the compounds based on portioning between solution and solid in the gels. The more hydrophobic and less soluble the compound, the more of it that is likely to be included into the solid component of the gel, thus increasing the "volume" of the solid network and potential gel strength as measured by rheology. This trend is, however, broken with the 2Cl-Phe and Br-Phe gels. This can be partly explained by the crystallography of the structures which is described below. In essence the structures start to significantly change with these halogen additions.

Crystallography studies

Crystal Structures

The gelation processes can often be better understood by determination of the solid state component of the colloidal material. Although often not possible, many supramolecular chemistry studies have turned to crystallography to gain insights into the interactions between the gelator molecules. Although a legitimate methodology, there are caveats to the method and the findings should always be taken with caution. However, hydrogelation by Phe and its derivatives provides an excellent opportunity to study this solid state phase of the colloidal materials as the solid is crystalline in nature. This is not a unique phenomenon, but certainly is one that is rare.[11] As a result, we determined the crystal structures of the majority of the compounds and materials formed during these studies. The hydrogels and water-based experiments all resulted in crystalline phases as confirmed by single crystal (Table 2) and PXRD data (Figs. S4-S10). The single crystal data were obtained

View Article Online
DOI: 10.1039/C7FD00108H

Table 2. Crystallographic details for the hydrogels. All forms were found as monohydrates. The published structures of Phe.H_2O and I-Phe.H_2O monoclinic forms are also presented for clarity.

$C_9H_{11}NO_2{\cdot}H_2O$ *	$C_9H_{10}FNO_2{\cdot}H_2O$	$C_9H_9F_2NO_2{\cdot}H_2O$	$C_9H_{10}ClNO_2{\cdot}H_2O$	$C_9H_{10}BrNO_2{\cdot}H_2O$	$C_9H_{10}INO_2{\cdot}H_2O$[2]	$C_9H_{10}INO_2{\cdot}H_2O$
M_r = 183.20	M_r = 201.20	M_r = 219.19	M_r = 217.65	M_r = 262.11	M_r = 309.10	M_r = 309.10
Monoclinic, $P2_1$	Monoclinic, $P2_1$	Monoclinic, $P2_1$	Monoclinic, $P2_1$	Monoclinic, $P2_1$	Monoclinic, $P2_1$	Orthorhombic, $P2_12_12_1$
a = 13.1117 (14) Å	a = 13.3028 (14) Å	a = 13.100 (3) Å	a = 13.5539 (8) Å	a = 6.3036 (4) Å	a = 6.2312 (5) Å	a = 5.3139 (3) Å
b = 5.4092 (5) Å	b = 5.4628 (6) Å	b = 5.4019 (12) Å	b = 5.4096 (3) Å	b = 5.3042 (3) Å	b = 5.2898 (4) Å	b = 6.3152 (4) Å
c = 13.8490 (14) Å	c = 14.0151 (15) Å	c = 14.423 (4) Å	c = 15.0157 (9) Å	c = 15.9161 (9) Å	c = 16.4690 (13) Å	c = 32.741 (2) Å
β = 102.985 (4)°	β = 104.048 (5)°	β = 100.712 (8)°	β = 108.421 (6)°	β = 97.947 (3)°	β = 96.772 (4)°	
V = 957.11 (17) Å^3	V = 988.02 (18) Å^3	V = 1002.8 (4) Å^3	V = 1044.56 (11) Å^3	V = 527.05 (5) Å^3	V = 539.06 Å^3	V = 1098.72 (12) Å^3
Z = 4	Z = 4	Z = 4	Z = 4	Z = 2	Z = 2	Z = 4
D_x = 1.271 Mg m^{-3}	D_x = 1.353 Mg m^{-3}	D_x = 1.452 Mg m^{-3}	D_x = 1.384 Mg m^{-3}	D_x = 1.652 Mg m^{-3}	D_x = 1.904 Mg m^{-3}	D_x = 1.869 Mg m^{-3}
Mo $K\alpha$ radiation, λ = 0.71073 Å	Mo $K\alpha$ radiation, λ = 0.71073 Å	Mo $K\alpha$ radiation, λ = 0.71073 Å	Cu $K\alpha$ radiation, λ = 1.54184 Å	Mo $K\alpha$ radiation, λ = 0.71073 Å		Mo $K\alpha$ radiation, λ = 0.71073 Å
Cell parameters from 4775 reflections	Cell parameters from 9917 reflections	Cell parameters from 2351 reflections	Cell parameters from 2578 reflections	Cell parameters from 8473 reflections		Cell parameters from 9924 reflections
θ = 2.4–26.6°	θ = 2.4–32.8°	θ = 2.9–24.0°	θ = 3.1–71.9°	θ = 2.6–32.1°		θ = 3.3–32.4°
T = 100 K	T = 100 K	T = 100 K	T = 120 K	T = 100 K	T = 103 K	T = 100 K
Needle, clear colourless	Needle, colourless	Needle, clear colourless	Needle, clear colourless	Needle, colourless	Needle, colourless	Needle, colourless
0.3 × 0.2 × 0.05 mm	0.4 × 0.4 × 0.1 mm	1 × 0.2 × 0.05 mm	0.4 × 0.1 × 0.01 mm	0.55 × 0.25 × 0.05 mm		0.4 × 0.25 × 0.1 mm

* published in another submitted paper from the same research groups.

by removing single fibrous crystals from the gel solutions. All these crystal forms were found to be hydrates (the 2Cl-Phe and 5F-Phe phases are yet to be determined). The F-Phe, 2F-Phe, Cl-Phe gel forming phases were all found to be isostructural in nature to the known form of Phe·monohydrate and the published structure of 3-fluorophenylalanine monohydrate.[2] This can be best evidenced by looking at their crystallographic details (Table 2), comparing their packing motifs (Fig. 6 and Figs. S11-S14) and comparing the molecular conformations (Fig. 7). The crystal structures of the Br-Phe and I-Phe single crystals will be discussed later as they are different. But firstly, the isostructurality of the gel forming crystals allows for analysis of the predominant interactions and the variations with different halogen additions. The packing motif of the crystal structures determined for nearly all the Phe derivatives contain a distinct AB bilayered pattern of a hydrophobic layer consisting of the phenyl groups, and a hydrophilic layer consisting of hydrogen bonding and electrostatic interactions between the negatively charged carboxylate groups and positively charged ammonium cation groups, which together form the zwitterionic component of the amino acids (Fig. 6). We note at this point that we determined the Phe.monohydrate crystal structure to be the thermodynamically most stable form in the presence of water.[1p] In the examples presented here, the bilayer arrangement is found in all the materials. The anisotropic assembly resulting in the fibre formation is through the electrostatic interactions of

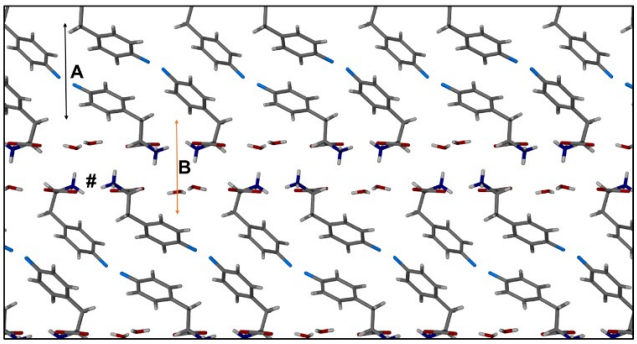

Fig. 6. A typical packing motif of the Phe derivatives. In this figure the packing of F-Phe is shown, with molecules shown in capped-stick representation. **A** (hydrophobic) and **B** (hydrophilic) layers are indicated. **#** is highlighting the dimer formation between the zwitterionic groups of the Phe molecules.

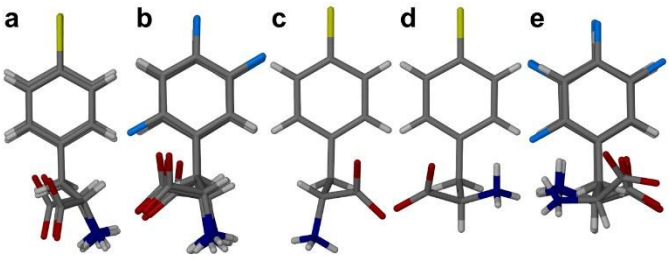

Fig. 7. Conformations of Phe and its derivatives in the monohydrate crystal structures. The crystal structures shown are the seven presented in Table 2, and the published EXAXIG and EXAXAC structures. The conformations of the Br-Phe and I-Phe structures (three conformations shown in (**a**)) are different to the conformations of the fluorinated and chlorinated Phe derivatives (**b** –**e**). The isostructural hydrates formed by the fluorinated and chlorinated Phe derivatives have a Z′ = 2, resulting in two distinct conformations (**b**-**c** and **d**-**e**). The difference between the fluorinated (*L*-configuration) and chlorinated (*D*-configuration) samples is the chirality. The 2,4,5-trifluoro-Phe derivative has one conformation that is the same as the others (**b**) and one that is slightly different (**e**).

the positive and negative components of the Phe derivatives down the b axis of all the structures. This is evident in all the structures found and reported here. With this in mind, the conformations of the Phe molecules within each of the structures were compared with the known Phe monohydrate, 3-fluorophenylalanine monohydrate, and 2,4,5-trifluorophenylalanine structures.[2] As can be seen in Fig. 7, the conformations of all the structures are relatively similar. The Z′ = 2 character results in two conformations in each structure, except for the Br-Phe and two I-Phe structures which has one conformation (Z′ = 1). For those three structures with Br-Phe and I-Phe the conformations are very similar to each other, and only slightly different from one of the conformations of the other structures. This gives clear evidence that the molecules with the Br-Phe and I-Phe structures prefer to be in this one conformation overall due to some increased interaction beyond the "hydrophilic" region of the Phe derivatives, i.e. hydrogen bonding, conformations and electrostatic interactions do not vary significantly within the structures and derivatives. This can be confirmed through the determination of the interactions of the structures through analyses of the electrostatic potentials and inter-atom distances.[12]

We previously reported that the intermolecular interactions in the Phe·monohydrate structure are dominated by the electrostatic interactions. Hirshfeld surface analyses of the structures reveal there are no significant changes in the interactions between the molecules when it comes to the hydrogen bonding and electrostatic interactions (Error! Reference source not found.). The clear difference occurs in the hydrophobic region of the phenyl groups. The fluoro groups appear only to increase the polarisation of the aromatic group and do not interact with each other significantly. Increased fluorination escalates the polarisation of the aromatic group and causes disruption of the hydrophobic packing motif, as seen in the 2,4,5-trifluorophenylalanine monohydrate structure. The chloro groups of the Cl-Phe monohydrate structure are interacting with each other. Two distances between chloro atoms can be discerned, 3.294(4) Å and 3.810(4) Å. The carbon-donor–acceptor angle for the shorter contact is 148.6(3) °. With the angle being considerably less than the ideal linear arrangement for strong halogen – halogen bonds, we can ascertain that this Type I halogen – halogen interaction does not disrupt the hydrophilic layer interactions. This interaction corresponds well with the "sigma hole" visible within the electrostatic potential Hirshfeld surface (Fig. 8).

The Br-Phe monohydrate structure isolated from an aged hydrogel was found to be isostructural to the known I-Phe monohydrate form (we have designated this as monoclinic Form I).[5a] Comparison of these structures with the single crystal data obtained from the failed gelation experiments of I-Phe revealed a polymorphic form (I-Phe monohydrate orthorhombic Form II). This crystal form has a relatively simple difference in the form of a change in layer packing. The change is from a parallel motif to a polarised form of Br-Phe and the published monoclinic Form I, (Fig. 9), to a classic herringbone motif. All three structures contain Type II halogen – halogen interactions (Fig. 9).[4] The halogen – halogen interactions are more significant in these three structures when compared to the interactions found in the Cl-Phe structure. The angles and distances for the three structures are: 3.5458(3) Å and 174.41(6) ˚ for the Br-Phe structure; 3.7517(4) Å and 173.7(1) ˚ for the I-Phe monoclinic structure; 3.7790(8) Å and 173.3(2) ˚ for the I-Phe orthorhombic structure. The conformation of the Phe molecules in these structures gives rise to no π-π interactions.

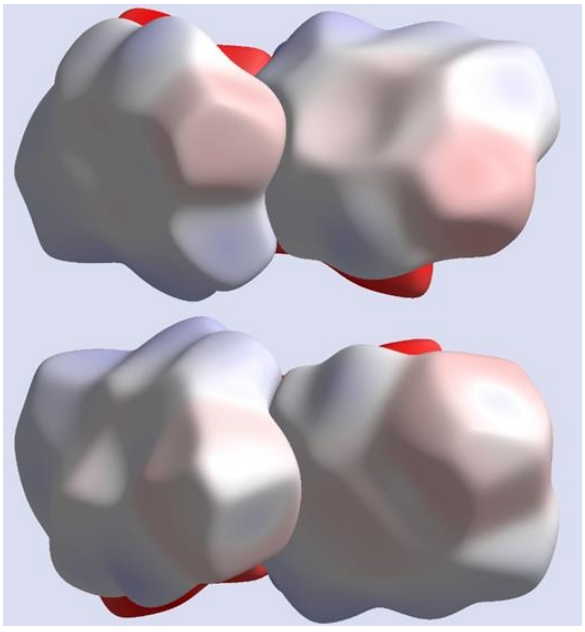

Fig. 8. Electrostatic potential Hirshfeld surfaces of the F-Phe (top) and Cl-Phe (bottom) derivatives within their asymmetric unit (ASU) of the respective monohydrate crystal structures. The halogenation of the aromatic ring results in increased polarisation of the hydrophobic groups and this can be viewed by the blue "hue" of the hydrogen edges of the aromatic groups and the red "hue" of the central carbon rings. The "sigma" hole of the chloro can be viewed in both molecules of the Cl-Phe ASU. This is the circular "white" region of the red area of the chloro groups.

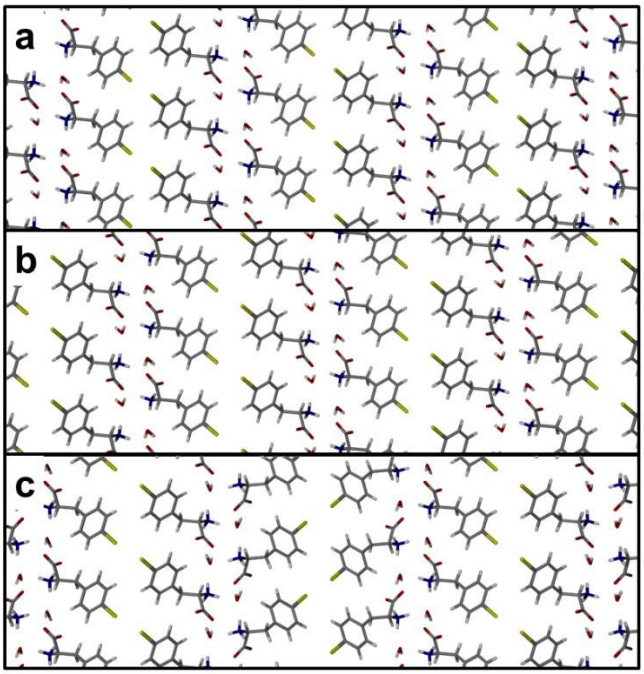

Fig. 8. Packing diagrams showing Br-Phe monohydrate (**a**), I-Phe monohydrate monoclinic Form I (**b**), and I-Phe monohydrate orthorhombic Form II (**c**).

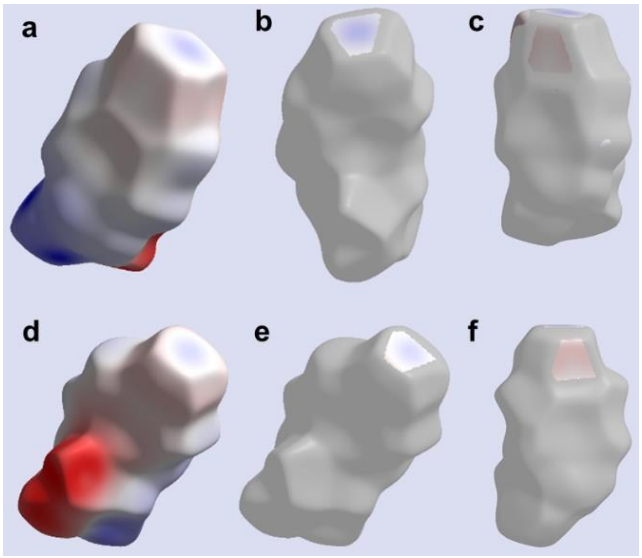

Fig. 10. Hirshfeld surfaces of the electrostatic potentials of the I-Phe (top) and Br-Phe (bottom) derivatives. The halogen – halogen interactions are shown clearly with the "sigma hole" indicated by the blue area (b and e) surrounded by white at the tips of the halogen groups. The sigma hole interacts with the electrostatically negative regions of the halogen groups perpendicularly, as you would expect for a Type II halogen – halogen interaction.

The electrostatic potential surface indicates the π negative potential that can interact with the electropositive potential of the C-H groups of the methylene group (Fig. S15). This is a common motif seen in all the structures of the monohydrates of the Phe derivatives.

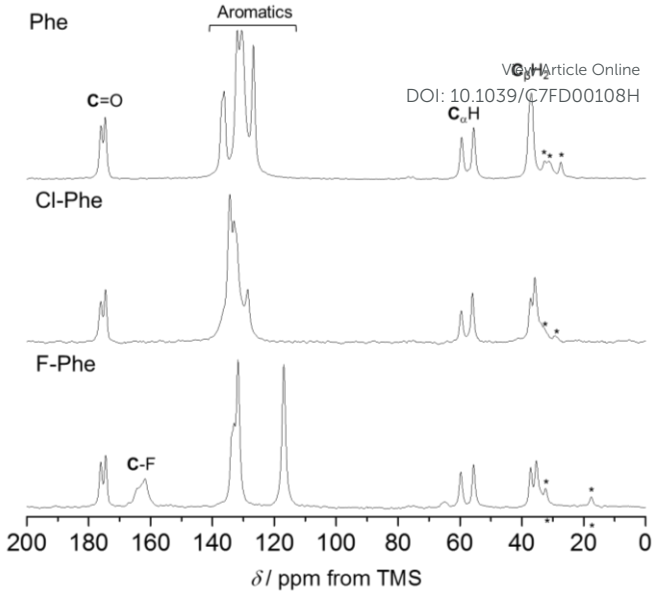

Fig. 9. ^{1}H-^{13}C CP/MAS NMR spectra of dry hydrogels of Phe, Cl-Phe and F-Phe (303 mM) acquired with an MAS rate of 10 kHz. * is highlighting spinning sidebands.

NMR studies

The supramolecular arrangement of the hydrogel fibres was investigated further using solid-state NMR spectroscopy. ^{1}H-^{13}C CP/MAS NMR spectra of Phe, Cl-Phe and F-Phe hydrogel samples, where the bulk water has been removed, showed two peaks per carbon site due to the presence of two magnetically non-equivalent molecular environments, which are in agreement with Z'=2 crystallographic information derived from monohydrate structures of Phe derivatives (Fig. 9). Strong dipolar interactions, chemical shift anisotropy and short transverse relaxation (T_2) processes characteristic of the rigid components are sources of significant peak broadening in ^{1}H solution-state NMR spectra of gels. However, Phe-based supramolecular gels do not require the whole population of gelator molecules to be incorporated in the gel network, as long as a certain concentration is reached to prompt spontaneous fibril formation.[13] Hence, a fraction of these molecules is dissolved in the isotropic phase (pools of solvent entrapped by the gel network) and is therefore "visible" to solution-state NMR spectroscopy.[14] The gel/solution exchange phenomenon characteristic of supramolecular gels enabled us to gain information about the organisation at the fibre/solution interfaces.

A clear difference in the relaxation times of different ^{1}H sites was observed in solutions of Phe, Cl-Phe and F-Phe (Fig. 10). Upon hydrogelation of Phe, ^{1}H T_1 times for different ^{1}H sites became similar, due to enhanced ^{1}H-^{1}H dipolar couplings resultant from restricted mobility of the gelator molecules. These data demonstrate that Phe gelator molecules are in the isotropic phase and exchange faster than the NMR frequency time scale while entrapped in the gel network.

Contrarily, the dispersion of ^{1}H T_1 values remained in hydrogels of Cl-Phe and F-Phe, despite fibre formation. This means that

mainly free gelator molecules were detected. This is a consequence of slower dynamics of exchange of Cl-Phe and F-Phe at the gel/solution interfaces, indicating the head substituent determines the strength of intermolecular interactions and dynamics of the molecular exchange at the interface. These phenomena are a subject of ongoing studies using advanced NMR methods and will be reported in another full paper.

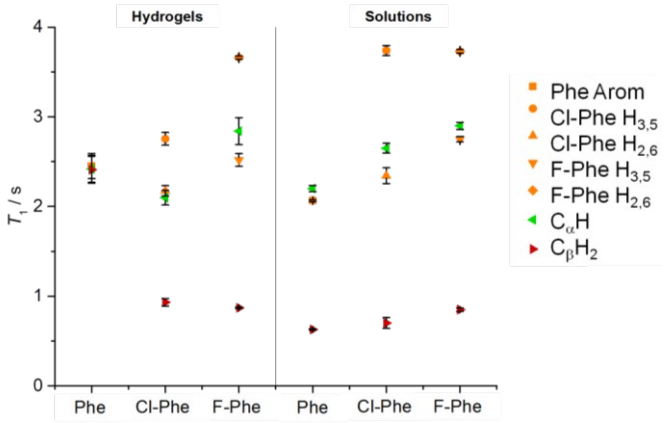

Fig. 10. ^{1}H longitudinal relaxation times (T_1) in hydrogels of Phe, Cl-Phe and F-Phe (303 mM). The small variations observed between gel and solutions of F-Phe were due to the overall rigidity imposed by the presence of an organised structure.

Conclusions

We have shown that halogenation of the aromatic ring of Phe can result in variation of the gelation properties in water and DMSO. Gelation in water results in crystalline phases and in a general improvement in gelation ability, due to a decrease in solubility, upon halogen addition. Analyses of the crystal structures reveal an isostructural behaviour with changes in the interactions between aromatic groups and halogen functionality driving changes in packing and therefore gelation functionality. This is in strong contrast to the FMOC-Phe halogen series of compounds that still shows gelation even though periodic crystalline packing changes upon addition of Br and I.[3] With an increase in the strength of the halogen – halogen interactions, the crystal packing motifs change, most notably when Br or I is positioned in the *para*-position of the aromatic group. This increased strength in the interactions is reflected by slower dynamics of exchange at the gel/solution interfaces. There is a stepped change with the addition of Br to the *para*-position on the aromatic group resulting in the gels becoming metastable. Indicating that the thermodynamically stable hydrate structure is no longer favoured, and becomes metastable. With the iodo functionality the gelation ability is lost and the monohydrate form shows polymorphism due to supramolecular isomerism.

Acknowledgements

GOL and YZK thank the EPSRC Directed Assembly network for funding. GOL, HGR and JSF thanks the Herchel Smith Fund (Cambridge), Heriot-Watt University and Royal Society of Edinburgh/Scottish Government for funding of fellowships. The EPSRC are thanked for DTP PH.D. studentships for HRG (EP/M507866/1). Prof. Bill Jones is thanked as host for GOL at Cambridge University. Mark Leonard and Jim Buckman (HWU) are thanked for their assistance with the SEM imaging. We are grateful for financial support from the University of East Anglia through fully funded Ph.D. studentships for KPN and SMR.

References

1 a) L. Adler-Abramovich, L. Vaks, O. Carny, D. Trudler, A. Magno, A. Caflisch, D. Frenkel and E. Gazit, *Nat. Chem. Biol.*, 2012, **8**, 701; b) T. D. Do, W. M. Kincannon and M. T. Bowers, *J. Am. Chem. Soc.*, 2015, **137**, 10080; c) S. Shaham-Niv, L. Adler-Abramovich, L. Schnaider and E. Gazit, *Sci. Adv.*, 2015, **1**, e1500137; d) V. Singh, R. K. Rai, A. Arora, N. Sinha and A. K. Thakur, *Sci. Rep.*, 2014, **4**, 3875; e) F. R. DePietro and J. D. Fernstrom, *Brain Res.*, 1999, **831**, 72; f) W.-P. Hsu, K.-K. Koo and A. S. Myerson, *Chem. Eng. Commun.*, 2002, **189**, 1079; g) T. Sato and C. Sano, *Method of obtaining phenylalanine anhydrous crystals*. EP 0703214 B1, 1995; h) E. Mossou, S. c. M. Teixeira, E. P. Mitchell, S. A. Mason, L. Adler-Abramovich, E. Gazit and V. T. Forsyth, *Acta Crystallogr. Sect. C Struct. Chem.*, 2014, **70**, 326; i) F. S. Ihlefeldt, F. B. Pettersen, A. von Bonin, M. Zawadzka and C. H. Görbitz, *Angew. Chem. Int. Ed.*, 2014, **53**, 13600; j) M. D. King, T. N. Blanton and T. M. Korter, *Phys. Chem. Chem. Phys.*, 2012, **14**, 1113; k) P. A. Williams, C. E. Hughes, A. B. M. Buanz, S. Gaisford and K. D. M. J. Harris, *Phys. Chem. C*, 2013, **117**, 12136; l) K. Yuyama, K. George, K. G. Thomas, T. Sugiyama and H. Masuhara, *Cryst. Growth Des.*, 2016, **16**, 953; m) J. Lu, J. Wang, Z. Li and S. Rohani, *African J. Pharm. Pharmacol.*, 2012, **6**, 269; n) R. Mohan, K. K. Koo, C. Strege and A. S. Myerson, *Ind. Eng. Chem. Res.*, 2001, **40**, 6111; o) B. Khawas, *Indian J. Phys. A*, 1985, **58**, 219; p) K. P. Nartowski, S. M. Ramalhete, P. C. Martin, J. S. Foster, M. Heinrich, M. D. Eddleston, H. R. Green, G. M. Day, Y. Z. Khimyak and G. O. Lloyd, *Cryst. Growth Des.*, 2017, submitted; q) E. C. Griffith and V. Vaida, *J. Am. Chem. Soc.*, 2013, **135**, 710.

2 a) Y. In, S. Kishima, K. Minoura, T. Nose, Y. Shimohigashi and T. Ishida, *Chem. Pharm. Bull.*, 2003, **51**, 1258; b) Y. Hiyama, J. V. Silverton, D. A. Torchia, J. T. Gerig and S. J. Hammond, *J. Am. Chem. Soc.*, 1986, **108**, 2715.

3 a) D. M. Ryan, S. B. Anderson and B. L. Nilsson, *Soft Matter*, 2010, **6**, 3220; b) W. Liyanage and B. L. Nilsson, *Langmuir*, 2016, **32**, 787; c) A. Pizzi, L. Lascialfari, N. Demitri, A. Bertolani, D. Maiolo, E. Carretti and P. Metrangolo, *CrystEngComm*, 2017, **19**, 1870.

4 a) G. R. Desiraju, P. S. Ho, L. Kloo, A. C. Legon, R. Marquardt, P. Metrangolo, P. Politzer, G. Resnati and K. Rissanen, *Pure Appl. Chem.*, 2013, **85**, 1711; b) G. Cavallo, P. Metrangolo, R. Milani, T. Pilati, A. Priimagi, G. Resnati and G. Terraneo, *Chem. Rev.*, 2016, **116**, 2478; c) H. Takezawa, T. Murase, G. Resnati, P. Metrangolo and M. Fujita, *Angew. Chem. Int. Ed.*, 2015, **54**, 8411; d) F. M. A. Noa, S. A. Bourne and L. R. Nassimbeni, *Cryst. Growth Des.*, 2015, **15**, 3271; e) A. Priimagi, G. Cavallo, P. Metrangolo and G. Resnati, *Acc. Chem. Res.*, 2013, **46**, 2686; f) A. Mukherjee, S. Tothadi and G. R. Desiraju, *Acc. Chem. Res.*, 2014, **47**, 2514; g) P. Politzer, P. Lane, M. C. Concha, Y. Ma and J. S. Murray, *J. Mol. Model.*, 2007, **13**, 305; h) J. D. Dunitz, *IUCrJ*, 2015, **2**, 157; i) G. R. Desiraju and R. Parthasarathy, *J. Am. Chem. Soc.*, 1989, **111**, 8725; j) P. Metrangolo and G. Resnato, *IUCrJ*, 2014, **1**, 5; k) P. Metrangolo, F. Meyer, T. Pilati,

View Article Online
DOI: 10.1039/C7FD00108H

G. Resnati and G. Terraneo, *Angew. Chem. Int. Ed.*, 2008, **47**, 6114.

5 a) A. Bertolani, L. Pirrie, L. Stefan, N. Houbenov, J. S. Haataja, L. Catalano, G. Terraneo, G. Giancane, L. Valli, R. Milani, O. Ikkala, G. Resnati and P. Metrangolo, *Nat. Commun.*, 2015, **6**:7574; b) A. N. Khan, M. Schmultz, J. Lacava, A. A. Ouahabi, T.-T.-T. Nguyen, P. J. Mesini and J.-M. Guenet, *Langmuir*, 2015, **31**, 7666; c) A. P. Piccionello, A. Guarcello, A. Calabrese, I. Pibiri, A. Pace and S. Buscemi, *Org. Biomol. Chem.*, 2012, **10**, 3044; d) Y. Feng, H. Chen, Z.-X. Liu, Y.-M. He and Q.-H. Fan, *Chem. Eur. J.*, 2016, **22**, 4980; e) S. H. Jungbauer, D. Bulfield, F. Kniep, C. W. Lehmann, E. Herdtweck and S. M. Huber, *J. Am. Chem. Soc.*, 2014, **136**, 16740; f) L. Meazza, J. A. Foster, K. Fucke, P. Metrangolo, G. Resnati and J. W. Steed, *Nature Chem.*, 2013, **5**, 42.

6 a) L. Wang, W. Qu, B. P. Lieberman K. Plössl and H. F. Kung, *Nucl. Med. Biol.*, 2011, **38**, 53; b) C. Huan, L. Yuan, K. M. Rich and J. McConathy, *Nucl. Med. Biol.*, 2013, **40**, 498.

7 R. R. Ernst, G. Bodenhausen and A. Wokaun, *Principles of nuclear magnetic resonance in one and two dimensions*, 1987, Clarendon Press Oxford: Vol. 14.

8 a) Y. Lan, M. G. Corradini, R. G. Weiss, S. R. Raghavan and M. A. Rogers, *Chem. Soc. Rev.*, 2015, **44**, 6035; b)

9 a) S. Abbott and C. Hansen, *Hansen Solubility Parameters in Practice*, 2015, Hansen-Solubility, eBook, ISBN: 9780955122026; b) C. Hansen, Hansen solubility parameters: a user's handbook, 2007, CRC Press.

10 R. G. Larson, *The Structure and Rheology of Complex Fluids*, 1999, Oxford University Press, Oxford.

11 a) E. Ostuni, P. Kamaras and R. G. Weiss, *Angew. Chem. Int. Ed. Engl.*, 1996, **35**, 1324; b) H. Shigemitsu, I. Hisaki, E. Kometani, D. Yasumiya, Y. Sakamoto, K. Osaka, T. S. Thakur, A. Saeki, S. Seki, F. Kimura, T. Kimura, N. Tohnai and M. Miyata, *Chem. Eur. J.*, 2013, **19**, 15366; c) K. M. Anderson, G. M. Day, M. J. Paterson, P. Byrne, N. Clarke and J. W. Steed, *Angew. Chem. Int. Ed.*, 2008, **47**, 1058; d) M. George, G. Tan, V. T. John and R. G. Weiss, *Chem. Eur. J.*, 2005, **11**, 3243.

12 a) G. Nandi and I. Goldberg, *CrystEngComm*, 2014, **16**, 8327; b) A. D. Martin, J. Britton, T. L. Eusan, A. J. Blake, W. Lewis and M. Schröder, *Cryst. Growth Des.*, 2015, **15**, 1697.

13 S. Bouguet-Bonnet, M. Yemloul and D. Canet, *J. Am. Chem. Soc.*, 2012, **134**, 10621.

14 S. M. Ramalhete, K. P. Nartowski, N. Sarathchandra, , J. Angulo, G. O. Lloyd & Y. Z. Khimyak, *Chem. Eur. J.*, 2017, DOI: 10.1002/chem.201700793.